J. Appl. Comput. Mech., 4(4) (2018) 286-298
DOI: 10.22055/JACM.2018.24272.1180

ISSN: 2383-4536
jacm.scu.ac.ir

Journal of
Applied and Computational Mechanics

Research Article

Free Convection Flow of an Electrically-Conducting Micropolar Fluid between Parallel Porous Vertical Plates Using Differential Transform

J.C. Umavathi[1], Ali J. Chamkha[2,3], M. Shekar[1]

[1] Department of Mathematics, Gulbarga University, Gulbarga Karnataka-585 106, India

[2] Mechanical Engineering Department, Prince Sultan Endowment for Energy and Environment, Prince Mohammad Bin Fahd University, Al-Khobar 31952, Saudi Arabia

[3] RAK Research and Innovation Center, American University of Ras Al Khaimah, United Arab Emirates

Received December 01 2017; Revised January 30 2018; Accepted for publication February 20 2018.
Corresponding author: Ali J. Chamkha, achamkha@pmu.edu.sa

Abstract. In the present study, the effect of temperature-dependent heat sources on the fully developed free convection flow of an electrically conducting micropolar fluid between two parallel porous vertical plates in the presence of a strong cross magnetic field is analyzed. The micropolar fluid fills the space inside the porous plates when the rate of suction at one boundary is equal to the rate of injection at the other boundary. The coupled nonlinear governing differential equations are solved using the differential transform method (DTM). Moreover, the Runge-Kutta shooting method (RKSM), which is a numerical method, is used for the validity of DTM method and an excellent agreement is observed between the solutions of DTM and RKSM. Trusting this validity, the effects of Hartmann number, Reynolds number, micropolar parameter, and applied electric field load parameter are discussed on the velocity, microrotation velocity, and temperature. The skin friction, the couple stress, and Nusselt numbers at the plates are shown in graphs. It is observed that the Hartmann number and the micropolar parameter decreases the skin friction and the couple stress at both plates for suction and injection.

Keywords: Free convection, Micropolar fluid, Porous channel, Differential Transform method.

1. Introduction

The concept of micropolar fluid deals with a class of fluids that exhibit certain microscopic effects arising from the micromotions of the fluid elements. These fluids contain dilute suspension of rigid macromolecules with individual motions that support stress and body moments, and are influenced by spin inertia. Micropolar fluids are those which contain micro-constituents that can undergo rotation and the presence of which can affect the hydrodynamics of the flow so that it can be distinctly non-Newtonian. Eringen [1] developed a theory based on which the local effects arising from the microstructure and the intrinsic motion of the fluid elements should be taken into account. The theory is expected to provide a mathematical model for the non-Newtonian fluid behavior observed in certain man-made liquids such as polymers, lubricants, fluids with additives, paints, animal blood, colloidal and suspension solutions, etc. The presence of dust or smoke, particularly in a gas, may also be modeled using micropolar fluid dynamics. Later, Eringen [2] extended the theory of thermo-micropolar fluids and derived the constitutive laws for fluids with microstructures. Interesting aspects of the theory and applications of micropolar fluids are addressed in the books by Lukasazewicz [3] and Eringen [4] in addition to the review article by Ariman et al. [5]. Agarwal and Dhanapal [6] analyzed the effect of temperature dependent heat sources on the fully developed free convection micropolar

Published Online: October 08 2018

fluid flow when a constant suction (or injection) is applied on the plates and the fluid. Srinivasacharya et al. [7] studied the effects of microrotation and frequency parameters on an unsteady flow of micropolar fluid between two parallel porous plates with a periodic suction. El-Amin [8, 9] obtained numerical solutions for problems of the steady free convection and the mass transfer flow in a micropolar fluid with a constant suction and studied the combined effect of internal heat generation and magnetic field. The problem of convective heat transfer for a micropolar fluid in the presence of uniform magnetic field was investigated by Emad et al. [10]. Joneidi et al. [11] discussed the micropolar fluid in a porous channel using Homotopy analysis method. Prathap Kumat et al. [12] studied the fully-developed laminar free-convection flow in a vertical channel with one region filled with a micropolar fluid and the other region with a viscous fluid. Recently, Mahmood and Sajid [13] studied the numerical solution for a steady flow of a micropolar fluid between two porous plates using the finite element method.

When the magneto-hydrodynamic effects are added to the microrotation, an interesting new problem arises due to several engineering applications such as in MHD generators, designing cooling system for nuclear reactors, flow meters, etc. where the microconcentration provides an important parameter for deciding the rate of heat flow; by simulating it, one can obtain the desired temperature in such equipment. Several investigations have been conducted on the theoretical and experimental studies of the micropolar flow in the presence of a transverse magnetic field during the last four decades. El-Haikem et al. [14] studied the Joule heating effects on magnetohydrodynamic free convection flow of a micropolar fluid. El-Amin [15] studied the magnetohydrodynamic free convection and the mass transfer flow in the micropolar fluid with a constant suction. Bhargava et al. [16] obtained a numerical solution for a free convection MHD micropolar fluid flow between two parallel porous vertical plates using the quasi-linearization method. The study conducted by Zueco et al. [17] addressed the unsteady free convection flow of an incompressible electrically conducting micropolar fluid bounded by two parallel infinite porous vertical plates applied to an external magnetic field and the thermal boundary condition of the forced convection. Umavathi et al. [18] investigated the magnetohydrodynamic Poiseuille-Couette flow and heat transfer in an inclined channel. Recently, Akinshilo et al. [19] have investigated the flow and heat transfer analysis of the Sodium Alginate Conveying Copper Nanoparticles between two parallel plates. Akinshilo and Sobamowo [20] also studied perturbation solutions for the study of MHD blood as a Third Grade Nanofluid transporting Gold Nanoparticles through a porous channel. The effect of variable thermal expansion coefficient and nanofluid properties on a steady natural convection in an enclosure was discussed by Ghahremani et al. [21]. Aminreza et al. [22] analyzed the partial slip boundary condition of nanofluids past a stretching sheet. The entropy analysis for nanofluid over a stretching sheet was also studied by Aminreza et al. [23]. In another study by Zargartalebi et al. [24], the effects of variable thermo physical properties on the convection boundary layer flow over a horizontal plate embedded in a porous medium and saturated with a nanofluid were observed. A new approach to the electrostatic pull-in instability of nanocantilever actuators using the ADM–Padé technique was published by Aminreza et al. [25].

One of the semi-analytical methods which does not need small parameters is the differential transform method (DTM). The concept of DTM was first presented by Zhou [26] for solving linear and nonlinear problems in electrical circuit problems. Chen and Ho [27] expanded this method for partial differential equations and Ayaz [28] applied it to the system of differential equations. This method constructs an analytical solution in the form of a polynomial, which is different from the traditional higher-order Taylor series method. The Taylor series method is computationally expensive for large orders. The differential transform method is an alternative procedure for obtaining an analytic Taylor series solution of differential equations. This method is well considered by many researchers [29-35].

In the present study, the effect of temperature-dependent heat sources on the fully developed free convection electrically conducting micropolar fluid between two parallel porous vertical plates in the presence of a strong cross magnetic field is analyzed using differential transformation method. The velocity, microrotation, and temperature functions are shown graphically and the effects of magnetic field and micropolar parameter are studied. The Runge–Kutta shooting method is used for the validation of the solutions obtained by DTM.

2. Mathematical formulation

Considering the fully developed steady, the laminar free convection flow of an incompressible micropolar fluid flows between two infinite parallel porous flat plates, kept at a distance h, through which fluid is uniformly injected or removed with speed V_0. The schematic diagram is shown in Fig. 1. The plates are maintained at constant temperatures, T_1 and T_2, in the presence of a strong magnetic field B_0 applied normal to the plates and an electric field E_0 applied parallel to the porous plates. The X-axis is taken along the plates and Y-axis is normal to them. Since the boundaries in the X-direction are of infinite dimensions, without any loss of generality, we assume that the physical quantities such as velocity, microrotation, and temperature depend on only Y. The velocity field is taken to be $(U, V, 0)$ and microrotation as $(0, 0, N)$.

It is assumed that the fluid possesses constant properties except the density variation due to temperature difference in the buoyancy term. The relevant equations governing the conservation of mass, momentum, microrotation, and energy are as follows [6, 16]:

$$\rho V_0 \frac{\partial U}{\partial Y} = (\mu + K)\frac{\partial^2 U}{\partial Y^2} + K\frac{\partial N}{\partial Y} + \rho g - \frac{\partial P}{\partial X} - \sigma_e B_0^2 U - \sigma_e B_0 E_0 \tag{1}$$

$$\rho j V_0 \frac{\partial N}{\partial Y} = \gamma \frac{\partial^2 N}{\partial Y^2} - K\left(2N + \frac{\partial N}{\partial Y}\right) \tag{2}$$

$$\rho C_p V_0 \frac{\partial T}{\partial Y} = K_f \frac{\partial^2 T}{\partial Y^2} + (\mu + K)\left(\frac{\partial U}{\partial Y}\right)^2 + \gamma\left(\frac{\partial N}{\partial Y}\right)^2 + 2K\left(N^2 + N\frac{\partial U}{\partial Y}\right) + \gamma_0 V_0 (T - T_0) \tag{3}$$

where the elements are defined as follows: ρ, the density; μ, the viscosity of the fluid; K, the gyroviscosity; g, the acceleration due to gravity; P, the pressure; σ_e, the electrical conductivity of the fluid; j, the micro-inertia density; γ, material constant; C_p, the specific heat at constant pressure; K_f, the thermal conductivity; γ_0, the constant of proportionality; $\gamma_0 V_0 (T - T_0)$ the amount of heat generated per unit volume in unit time as a linear function of temperature; T_0, the temperature in hydrostatic state.

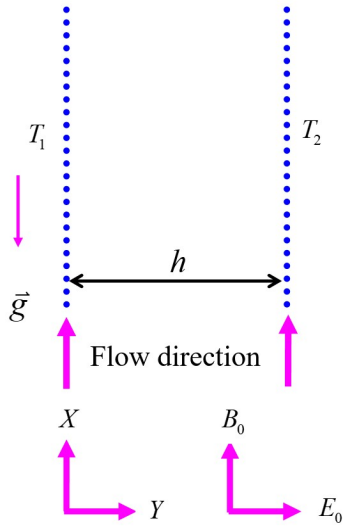

Fig. 1. Physical model and the coordinate system

Compared with Newtonian fluids, the governing equations include the microrotation or the angular velocity N whose direction of rotation is in the XY -plane and the material parameters j and γ. In order to be consistent with other micropolar studies, all material parameters are considered as independent and constant. The body force term is expressed as a buoyancy term,

$$\rho g - \frac{\partial P}{\partial X} = \rho\beta (T - T_0) f_X \tag{4}$$

where $f_X = -g$ and β is the coefficient of volumetric expansion. The boundary conditions are given by:

$$U = 0, \quad N = 0 \quad \text{at} \quad Y = 0, h \tag{5}$$

$$T = T_1 \quad \text{at} \quad Y = 0, \tag{6}$$

$$T = T_2 \quad \text{at} \quad Y = h$$

As the plates are infinitely long, the pressure P can be considered as equal to the hydrostatic pressure. Using Eq. (4), Eqs. (1-3) can be written as:

$$(\mu + K)\frac{d^2 U}{dY^2} - \rho V_0 \frac{dU}{dY} + K\frac{dv_3}{dY} + \rho\beta (T - T_0) f_X - (B_0 U + E_0)\sigma_e B_0 = 0 \tag{7}$$

$$\gamma\frac{d^2 v_3}{dY^2} - \rho j V_0 \frac{dv_3}{dY} - K\left(2v_3 + \frac{dU}{dY}\right) = 0 \tag{8}$$

$$K_f \frac{d^2 (T - T_0)}{dY^2} - \rho C_p V_0 \frac{d(T - T_0)}{dY} + (\mu + K)\left(\frac{dU}{dY}\right)^2 + \gamma\left(\frac{dv_3}{dY}\right)^2 + 2K\left(v_3^2 + v_3\frac{dU}{dY}\right) + \gamma_0 V_0 (T - T_0) = 0 \tag{9}$$

Introducing the dimensionless flow variables leads to:

$$y = \frac{Y}{h}, \quad u = \frac{\rho f_X \beta h^2}{K_f} U, \quad \theta = \frac{\rho^2 f_X^2 \beta^2 h^4}{K_f \mu}(T - T_0), \quad N = \frac{\rho f_X \beta h^3}{K_f} v_3, \quad \mathrm{Re} = \frac{\rho v_0 h}{\mu}, \quad M = \left(\frac{\sigma_e B_0^2 h^2}{\mu}\right)^{1/2},$$
$$E = \frac{E_0 \rho f_X \beta h^2}{\sigma_e B_0 K_f}, \quad R = \frac{K}{\mu}, \quad A = \frac{\gamma}{\mu h^2}, \quad \mathrm{Pr} = \frac{\mu C_p}{K_f}, \quad \gamma_1 = \frac{\gamma_0 h}{\rho C_p}, \tag{10}$$

where M is the Hartmann number, E is the electric load parameter, Pr is the Prandtl number, R is the micorpolar parameter, A and B are the micropolar material constants. By substituting Eq. (10) in the governing Eqs. (7-9) and after a little simplification, the following ordinary equations in the dimensionless form are obtained:

$$\frac{d^2u}{dy^2}-\frac{\mathrm{Re}}{1+R}\frac{du}{dy}+\frac{R}{1+R}\frac{dN}{dy}+\frac{\theta}{1+R}-\frac{M^2}{1+R}(u+E)=0 \tag{11}$$

$$\frac{d^2N}{dy^2}-\frac{\mathrm{Re}B}{A}\frac{dN}{dy}-\frac{R}{A}\left(2N+\frac{du}{dy}\right)=0 \tag{12}$$

$$\frac{d^2\theta}{dy^2}-\mathrm{Re}\,\mathrm{Pr}\frac{d\theta}{dy}+(1+R)\left(\frac{du}{dy}\right)^2+A\left(\frac{dN}{dy}\right)^2+2R\left(N+N\frac{du}{dy}\right)+\gamma_1\,\mathrm{Re}\,\mathrm{Pr}\,\theta=0 \tag{13}$$

As $\mathrm{Re}<0$, the problem corresponds to the injection at both walls and as $\mathrm{Re}>0$, it corresponds to the suction at both walls. The boundary conditions (5) and (6) for Eqs. (11-13) in the dimensionless form can be written as:

$$u=0,\quad N=0\quad \text{at}\quad y=0,1 \tag{14}$$

$$\begin{aligned}&\theta=q\quad \text{at}\quad y=0,\\ &\theta=\varepsilon q\quad \text{at}\quad y=1\end{aligned} \tag{15}$$

where $q=\mathrm{Pr}Gr\beta f_X h/C_p$ is the dimensionless parameter, $Gr=\rho^2\beta f_X h^3(T_1-T_0)/\mu^2$ is the Grashof number, and $\varepsilon=(T_2-T_0)/(T_1-T_0)$ is the non-dimensional heating parameter. The physical quantities of interest in this problem are the shear stress τ and the couple stresses m_w on the walls of the channel, which are defined as:

$$\tau=(1+R)\left.\frac{du}{dy}\right|_{y=0,1} \tag{16}$$

$$m_W=\left.\frac{dN}{dy}\right|_{y=0,1} \tag{17}$$

The other physical quantities of interest are the Nusselt number Nu at the walls of the channel, which can be defined as:

$$Nu=\begin{cases}-\dfrac{1}{q}\left.\dfrac{d\theta}{dy}\right|_{y=0,1}, & \text{for } \varepsilon=1\\[2ex] \dfrac{1}{(\varepsilon-1)q}\left.\dfrac{d\theta}{dy}\right|_{y=0,1}, & \text{for } \varepsilon\neq 1\end{cases} \tag{18}$$

3. Method of solution

3.1 Basic concepts of the differential transform method

The differential transformation of an analytical function $\bar{U}(k)$ is defined as follows (Zhou [26]):

$$\bar{U}(k)=\frac{1}{k!}\left[\frac{d^k u(y)}{dy^k}\right]_{y=0} \tag{19}$$

and the inverse differential transformation is given by

$$u(y)=\sum_{k=0}^{\infty}\bar{U}(k)y^k \tag{20}$$

Combining Eqs. (10) and (20) yields

$$u(y)=\sum_{k=0}^{\infty}\frac{y^k}{k!}\left.\frac{d^k u(y)}{dy^k}\right|_{y=0} \tag{21}$$

It can be seen in Eq. (20) that the differential transformation method is derived from Taylor's series expansion. In real applications, the sum $\sum_{k=n}^{\infty}\bar{U}(k)y^k$ is very small and can be neglected when n is sufficiently large. Therefore, $u(y)$ can be expressed by a finite series, and Eq. (21) is written as

$$u(y)=\sum_{k=0}^{n}\bar{U}(k)y^{k} \tag{22}$$

where the value of n depends on the convergence requirements in real applications and $\bar{U}(k)$ is the differential transform of $u(y)$. Table 1 lists the basic mathematics operations frequently used in the following analysis. Taking differential transform of Eqs. (11-13) into account, one can obtain the transformed equations as

$$\bar{U}(k+2)=\frac{1}{(1+R)(k+1)(k+2)}\left(\mathrm{Re}(k+1)\bar{U}(k+1)-R(k+1)\bar{N}(k+1)-\Theta(k)+M^{2}\left(\bar{U}(k)+E\,\delta(k)\right)\right) \tag{23}$$

$$\bar{N}(k+2)=\frac{1}{(k+1)(k+2)}\left(\frac{\mathrm{Re}\,B}{A}(k+1)\bar{N}(k+1)+\frac{2R\,\bar{N}(k)}{A}+\frac{R}{A}(k+1)\bar{U}(k+1)\right) \tag{24}$$

$$\begin{aligned}\Theta(k+2)=&\frac{1}{(k+1)(k+2)}\left(\mathrm{Re}\,\mathrm{Pr}(k+1)\Theta(k+1)-2R\,\bar{N}(k)-\gamma_{1}\,\mathrm{Re}\,\mathrm{Pr}\,\Theta(k)\right.\\&-(1+R)\sum_{r=0}^{k}(k-r+1)(r+1)\bar{U}(k-r+1)\bar{U}(r+1)-A\sum_{r=0}^{k}(k-r+1)(r+1)\bar{N}(k-r+1)\bar{N}(r+1)\\&\left.-2R\sum_{r=0}^{k}(k-r+1)\bar{U}(k-r+1)\bar{N}(r)\right)\end{aligned} \tag{25}$$

where $\delta(k)=\begin{cases}1 & \text{for } k=0\\ 0 & \text{for } k>0\end{cases}$, $\bar{U}(k)$, $\bar{N}(k)$, and $\Theta(k)$ are the transformed notations of $u(y)$, $N(y)$, and $\theta(y)$, respectively. The following relations are the transformed initial conditions:

$$\begin{aligned}&\bar{U}(0)=0,\ \bar{U}(1)=c_{1}\\&\bar{N}(0)=0,\ \bar{N}(1)=c_{2}\\&\Theta(0)=q,\ \Theta(1)=c_{3}\end{aligned} \tag{26}$$

Table 1. The operations for the one-dimensional differential transform method.

Original function	Transformed function
$y(x)=g(x)\pm h(x)$	$Y(k)=G(k)\pm H(k)$
$y(x)=\alpha g(x)$	$Y(k)=\alpha G(k)$
$y(x)=\frac{dg(x)}{dx}$	$Y(k)=(k+1)G(k+1)$
$y(x)=\frac{d^{2}g(x)}{dx^{2}}$	$Y(k)=(k+1)(k+2)G(k+2)$
$y(x)=g(x)h(x)$	$Y(k)=\sum_{l=0}^{k}G(l)H(k-l)$
$y(x)=x^{m}$	$Y(k)=\delta(k-m)=\begin{cases}1, \text{if } k=m\\ 0, \text{if } k\neq m\end{cases}$

Using the boundary condition (11), we can evaluate c_1, c_2 and c_3. Recurrence relations used in finding the solutions using DTM are as follows:

$$\begin{aligned}&U(0)=0;\\&U(1)=0.1478;\\&U(2)=\frac{-R\,N(1)-\theta(0)+M^{2}U(0)+E\,M^{2}+\mathrm{Re}\;U(1)}{2(1+R)};\\&N(0)=0;\\&N(1)=0.0876;\\&N(2)=\frac{B\;\mathrm{Re}\,N(1)+R\left(2N(0)+U(1)\right)}{2A};\end{aligned} \tag{27}$$

$$\theta(0) = q;$$
$$\theta(1) = 1.0847$$
$$\theta(2) = \frac{-A\left[N(1)\right]^2 - \text{Pr Re}\,\gamma_1\theta(0) + \text{Pr Re}\,\theta(1) - (1+R)\left[U(1)\right]^2 - 2R\left[\left[N(0)\right]^2 + N(0)U(1)\right]}{2}. \quad \text{(27-cont.)}$$

Higher order recurrence relations can be obtained easily by using Eqs. (23) to (25). By utilizing DTM and the transformed boundary conditions, the above-mentioned equations finally lead to the solution of a system of algebraic equations. For $M = \sqrt{5}$, $E = 1$, $\text{Re} = 2$, $R = 3$, $\text{Pr} = 0.733$, $A = 1$, $B = 0.001$, $\gamma_1 = 1$, $q = 1$ and $\varepsilon = 1$, we have found $c_1 = -0.41281159$, $c_2 = 0.201898003$ and $c_3 = 0.659387681$.

4. Results and Discussion

In the present study, the effect of temperature dependent heat sources on the fully developed free convection electrically conducting micropolar fluid between two parallel porous vertical plates in a strong cross magnetic field is analyzed. The governing equations are solved using DTM. The case of $E = 0$ corresponds the short circuit case and $E \neq 0$ corresponds to the open circuit case. To study the physical situation of this problem, we have computed the numerical values of the velocity, microrotation, and temperature in the channel and also find the skin friction, couple stress, and Nusselt number at the walls. The material constant γ_1 and the micropolar material constants A and B are taken to be constant as 1.0, 1.0, and 0.001, respectively. Whereas the effect of other important parameters, namely micropolar parameter *R*, Reynolds number Re, Hartmann number M^2, and Prandtl number Pr has been studied for these parameters and the corresponding profiles are shown in Figs. 2–10.

Table 2a. Values of $-u''(0)$ for different values of the Hartmann number M and micropolar parameter R for $E = 0$, $A = 1$, $B = 0.001$, $q = 1$, $\text{Pr} = 0.733$, $\varepsilon = 1$, $\gamma = 1$.

Re = –2					
M^2	$R = 3$	Bhargava et al.[16]	R	$M^2 = 5$	Bhargava et al.[16]
0	0.271355	0.270853	0	1.834443	1.744551
1	0.271052	0.268153	1	0.700700	0.648696
5	0.269979	0.260610	3	0.269979	0.260610
10	0.268881	0.254872	5	0.147928	0.152236
Re = 2					
0	0.135410	0.146179	0	0.411415	0.418457
1	0.138005	0.153360	1	0.284084	0.313665
5	0.147191	0.172302	3	0.147191	0.172302
10	0.156548	0.184977	5	0.083764	0.108876

Table 2b. Values of $\theta'(0)$ for different values of the Hartmann number M and micropolar parameter R for $E = 0$, $A = 1$, $B = 0.001$, $q = 1$, $\text{Pr} = 0.733$, $\varepsilon = 1$, $\gamma = 1$.

Re = –2					
M^2	$R = 3$	Bhargava et al.[16]	R	$M^2 = 5$	Bhargava et al.[16]
0	-0.796134	-0.777345	0	-0.782739	-0.768676
1	-0.796600	-0.778835	1	-0.641478	-0.777926
5	-0.798150	-0.782115	3	-0.798150	-0.782115
10	-0.799568	-0.783783	5	-0.800194	-0.783436
Re = 2					
0	0.639558	0.623848	0	0.644231	0.628725
1	0.638955	0.621962	1	0.637290	0.622106
5	0.636947	0.617790	3	0.636947	0.617790
10	0.635104	0.615644	5	0.634592	0.616200

Validity of the Differential Transform Method is shown in Tables 2a and 2b and 3. On the other hand, the present results for

the limiting case of $E = 0$ in addition to the DTM solution used herein are validated by comparing the values with previous results. Fifteen terms are taken into consideration while evaluating the solutions using DTM. Tables 2a and 2b show the comparison of the present study results with those of Bhargava et al. [16]. The results given in Tables 2a and 2b show an agreement to one decimal places. Moreover, the values of velocity u, microrotation N^*, and temperature θ obtained by DTM and RKSM solutions are shown in Table 3.

Table 3. Comparison results of velocity, microrotation, and temperature with RKSM for $M^2 = 5$, $\mathrm{Re} = 2$, $R = 3$, and $E = 0$

y	DTM			RKSM	Error
	5 terms	10 terms	15 terms		RKSM-DTM
			Velocity		
1	0	0	0	0	0.00E+00
0.9	0.01417910	0.01263415	0.01263506	0.01263506	0.00E+00
0.8	0.02454914	0.02234027	0.02234088	0.02234088	0.00E+00
0.7	0.03136758	0.02903311	0.02903320	0.02903320	0.00E+00
0.6	0.03487777	0.03272158	0.03272125	0.03272125	1.00E-08
0.5	0.03531561	0.03348893	0.03348836	0.03348836	0.00E+00
0.4	0.03291628	0.03147736	0.03147672	0.03147672	0.00E+00
0.3	0.02792090	0.02687650	0.02687592	0.02687593	0.00E+00
0.2	0.02058328	0.01991536	0.01991495	0.01991495	0.00E+00
0.1	0.01117658	0.01085763	0.01085742	0.01085742	0.00E+00
0	0	0	0	0	0.00E+00
			Microrotation		
1	0	0	0	0	0.00E+00
0.9	0.00484160	0.00425377	0.00425295	0.00425295	0.00E+00
0.8	0.00610238	0.00539152	0.00539042	0.00539043	1.00E-08
0.7	0.00495977	0.00438114	0.00438006	0.00438006	0.00E+00
0.6	0.00241174	0.00207147	0.00207055	0.00207055	0.00E+00
0.5	-6.87025E-4	-7.81598E-4	-7.82292E-4	-7.8229E-4	2.00E-09
0.4	-0.00358896	-0.00348943	-0.00348990	-0.00348989	1.00E-08
0.3	-0.00561741	-0.00540507	-0.00540533	-0.00540533	0.00E+00
0.2	-0.00613052	-0.00589716	-0.00589728	-0.00589728	0.00E+00
0.1	-0.00448501	-0.00432304	-0.00432306	-0.00432306	0.00E+00
0	0	0	0	0	0.00E+00
			Temperature		
1	1.00000000	1.00000000	1.00000000	1.00000000	0.00E+00
0.9	1.08867693	1.09066824	1.09057882	1.09057897	1.50E-07
0.8	1.15075402	1.15360852	1.15350203	1.15350218	1.50E-07
0.7	1.18899285	1.19200093	1.19190311	1.19190324	1.30E-07
0.6	1.20607232	1.20882105	1.20873922	1.20873932	1.00E-07
0.5	1.20457358	1.20685547	1.20679053	1.20679061	8.00E-08
0.4	1.18696492	1.18870783	1.18865879	1.18865885	6.00E-08
0.3	1.15558664	1.15680031	1.15676573	1.15676577	4.00E-08
0.2	1.11263593	1.11337317	1.11335156	1.11335159	3.00E-08
0.1	1.06015182	1.06048310	1.06047301	1.06047302	1.00E-08
0	1.00000000	1.00000000	1.00000000	1.00000000	0.00E+00

It can be found in Table 3 that an excellent agreement has been achieved between DTM and RKSM methods solutions. Table 3 also demonstrates the convergence rate of DTM. In general, fifteen terms of DTM approximation are sufficient to give a match with the numerical results to eight decimal places. This table shows that regarding these problem types, DTM converges more easily. The close correspondence between the present and numerical results lends further credibility to the methodology used in this study. Therefore, in summary, based on the aforementioned comparisons, DTM can achieve more satisfying results in predicting the solution of these types of problems. The present investigation is completed by depicting the

effects of some important parameters to evaluate how these parameters influence the fluid.

Figure 2 illustrates the effect of Hartmann number M^2 on the velocity for the short circuit $(E=\pm 1)$ and the open circuit $(E=0)$. Profiles are shown for both positive $\mathrm{Re}(=2)$ (i.e. for injection at $y=0$ and suction at $y=1$) and negative $\mathrm{Re}(=-2)$ (i.e. for suction at $y=0$ and injection at $y=1$). As the Hartmann number increases, the velocity decreases when $E=0$ and 1, whereas velocity increases when $E=-1$ for both suction and injection. The effect of a negative E is to add the flow while the effect of a positive E is to oppose the flow as compared to the case when $E=0$. It is observed that the velocity is more for suction and less for injection for both open and short circuits. In particular for $E=0$, velocity is more in the channel when there is injection at $y=0$ and suction at $y=1$ when compared to suction at $y=0$ and injection at $y=1$.

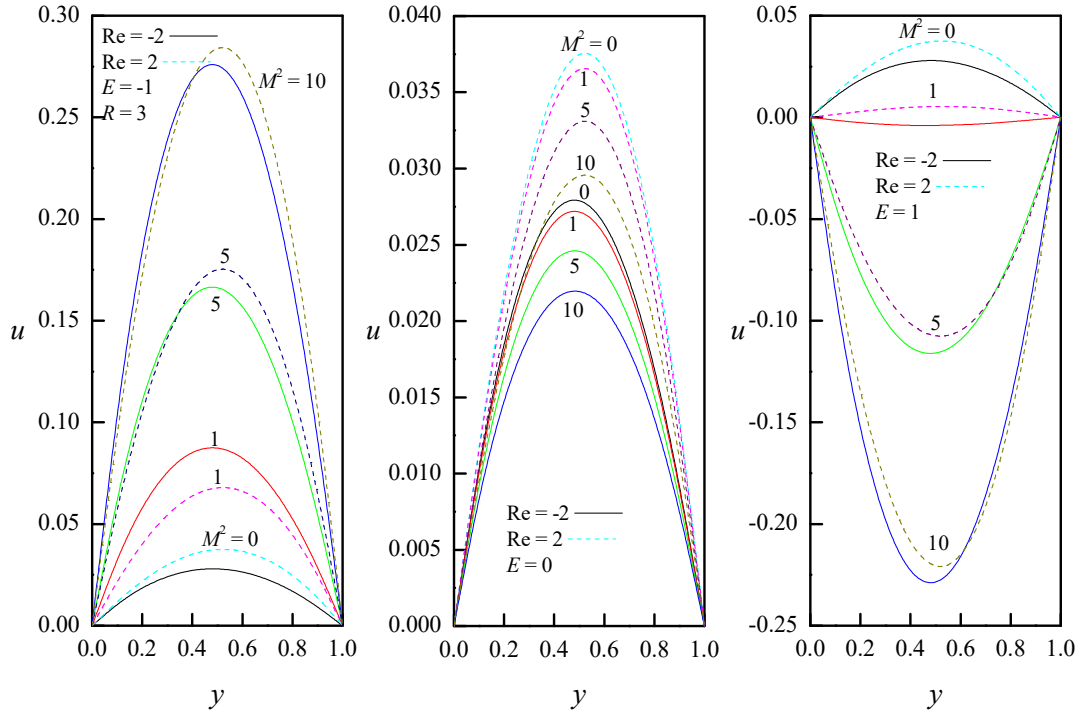

Fig. 2. Velocity profiles for different values of Hartmann number, electric load parameter, and Reynolds number with $R=3$, $A=1$, $B=0.001$, $q=1$, $\mathrm{Pr}=0.733$, $\varepsilon=1$, $\gamma=1$.

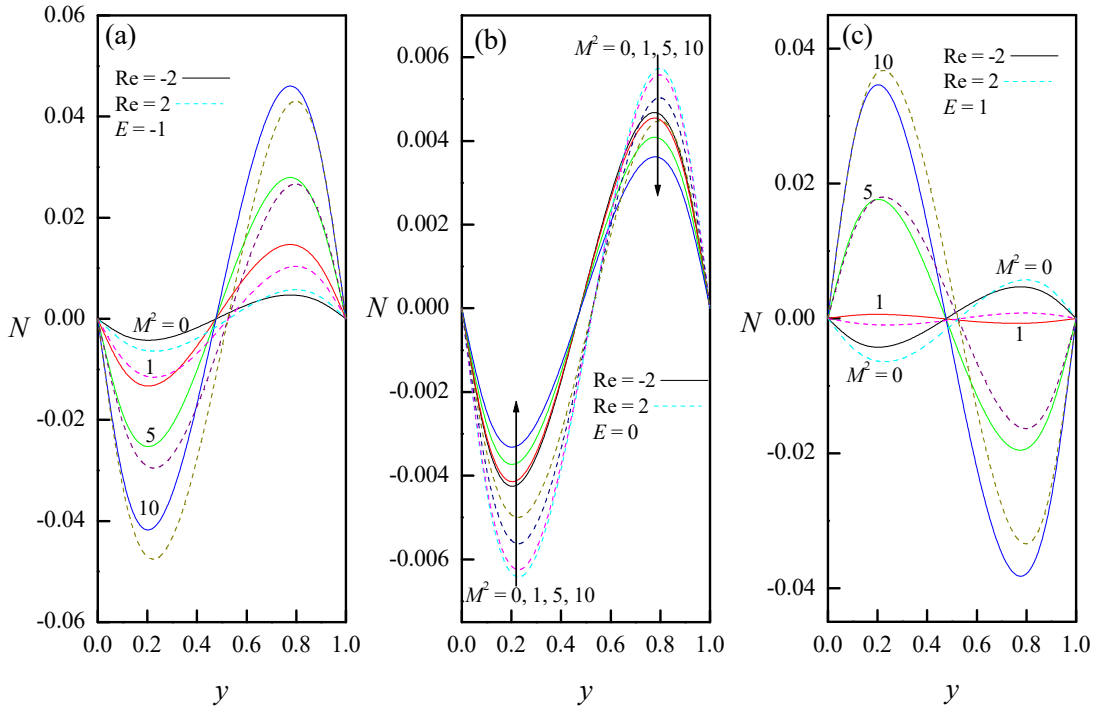

Fig. 3. Microrotation for different values of Hartmann number, electric load parameter, and Reynolds number with $R=3$, $A=1$, $B=0.001$, $q=1$, $\mathrm{Pr}=0.733$, $\varepsilon=1$, $\gamma=1$.

The effect of Hartmann number M^2 on the microrotation velocity N for the fixed $R=3$ is shown in Fig. 3. The microrotation velocity increases as the Hartmann number increases at $y=0$ and decreases at $y=1$ for the short circuit. But for the open circuit, the microrotation velocity decreases at $y=0$ and increases at $y=1$ when $E=-1$, whereas reversal effect is observed when $E=1$. It is also observed in Fig. 3a that the microrotation velocity enhances for injection and suppresses for suction when $E=-1$. But when $E=1$ the microrotation velocity enhances for suction and suppresses for injection as shown in Fig. 3b. The similar effect is noticed when $E=0$.

Figure 4 depicts the temperature profiles for different values of the Hartmann number M^2 and the electric load parameter E. For the open circuit, the effect of increasing Hartmann number is to decrease the temperature and for the short circuit the effect of Hartmann number is invariant on temperature. It is also observed that the effect of magnetic field for injection on temperature shows an increase in the upward direction, whereas for suction, it shows reduction in the downward direction of temperature distribution for the open circuit.

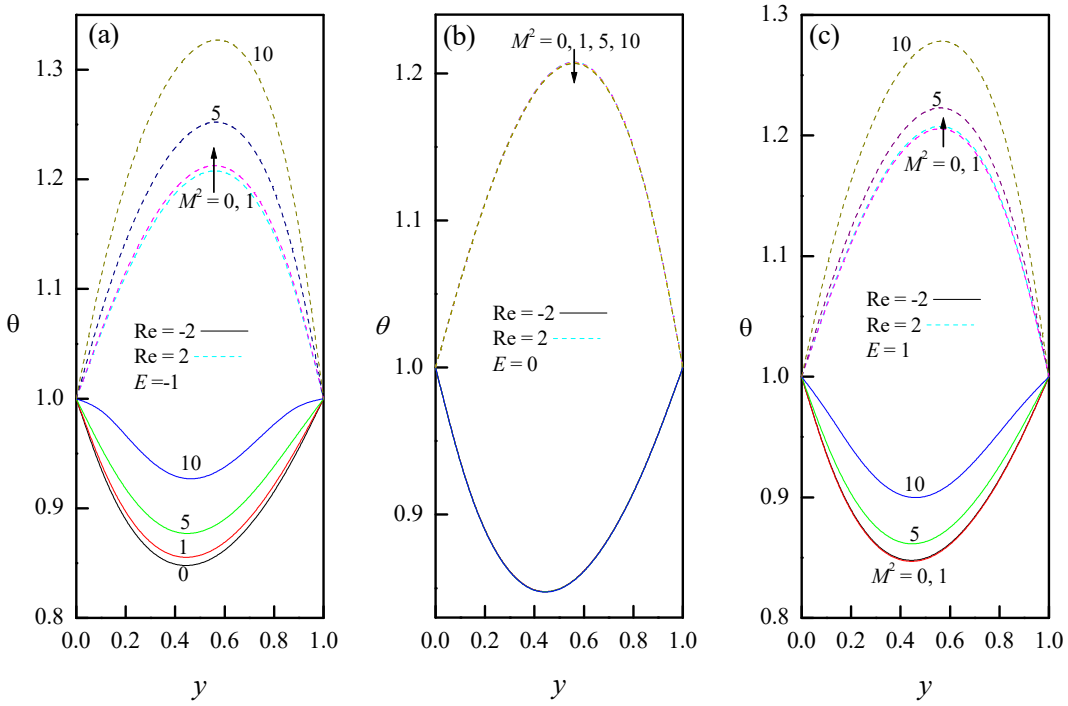

Fig. 4. Temperature for different values of Hartmann number, electric load parameter, and Reynolds number with $R=3$, $A=1$, $B=0.001$, $q=1$, $\mathrm{Pr}=0.733$, $\varepsilon=1$, $\gamma=1$.

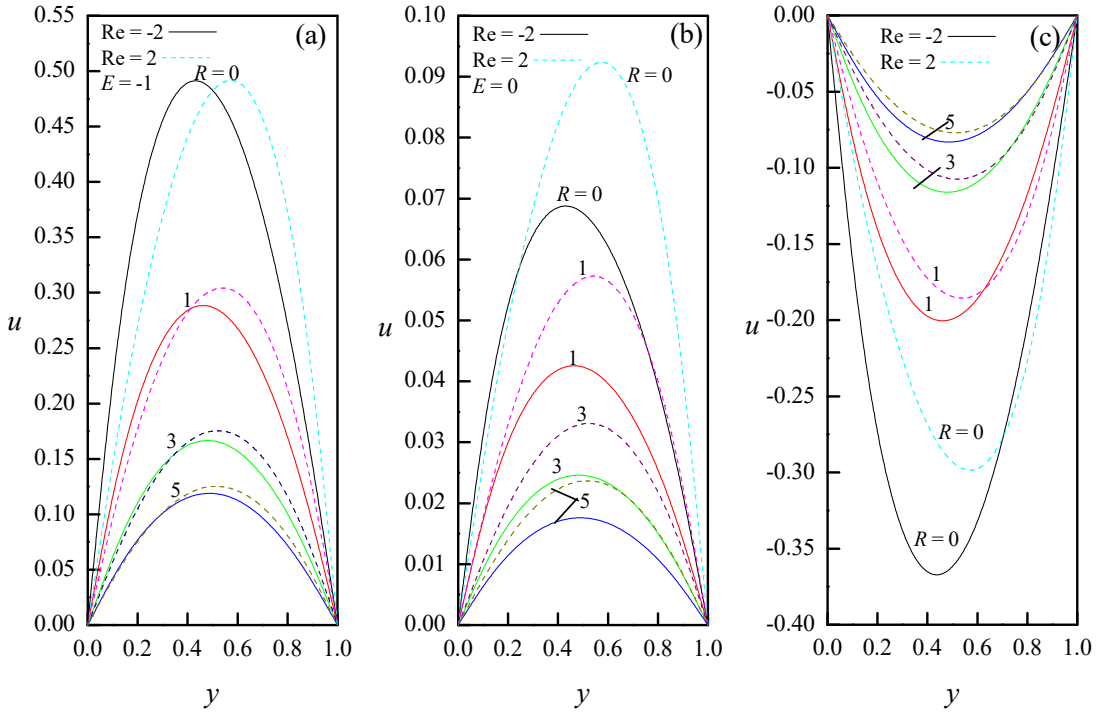

Fig. 5. Velocity profiles for different values of micropolar parameter, electric load parameter, and Reynolds number with $M^2=5$, $A=1$, $B=0.001$, $q=1$, $\mathrm{Pr}=0.733$, $\varepsilon=1$, $\gamma=1$.

The behavior of velocity field on the micropolar parameter and the electric load parameter for both suction and injection is shown in Fig. 5. As the micropolar parameter increases, the velocity decreases for $E=-1$ and 0 whereas it increases in downward direction for $E=1$. It is observed in Fig. 5 that the velocity is the same for injection and suction when $E=-1$ whereas the velocity is higher for suction as compared to injection for the short circuit $(E=0)$ as shown in Figs. 5(a, b). It is observed in Fig. 4c that when $E=1$, the velocity is higher for injection and lower for suction.

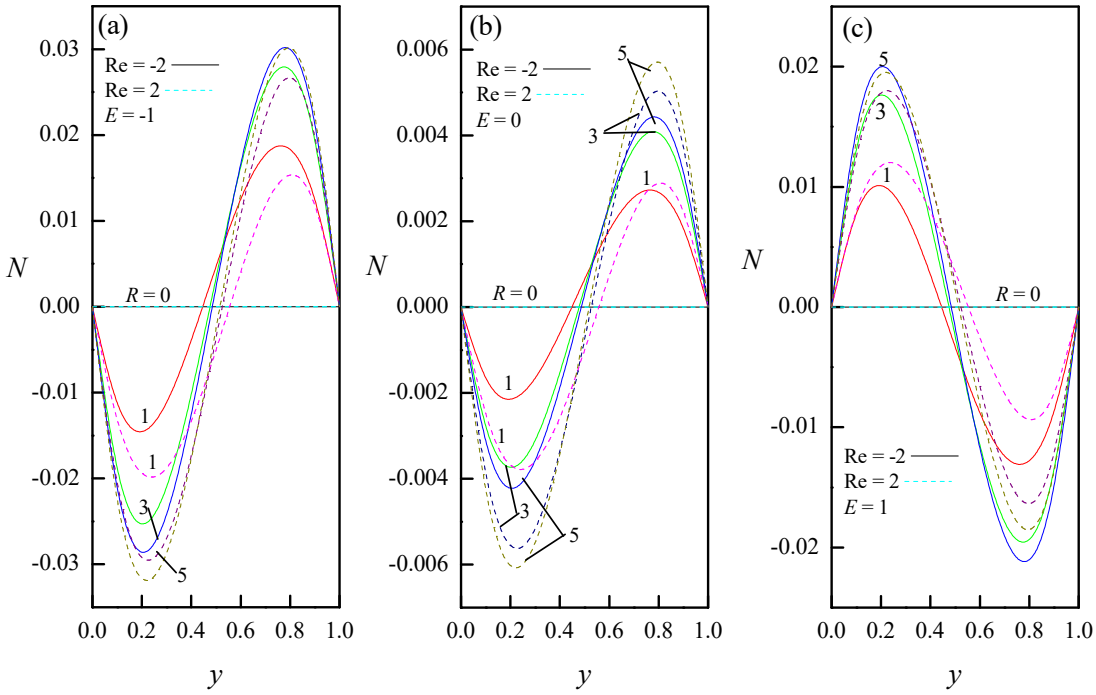

Fig. 6. Microrotation for different values of micropolar parameter, electric load parameter, and Reynolds number with $M^2=5$, $A=1$, $B=0.001$, $q=1$, $\mathrm{Pr}=0.733$, $\varepsilon=1$, $\gamma=1$.

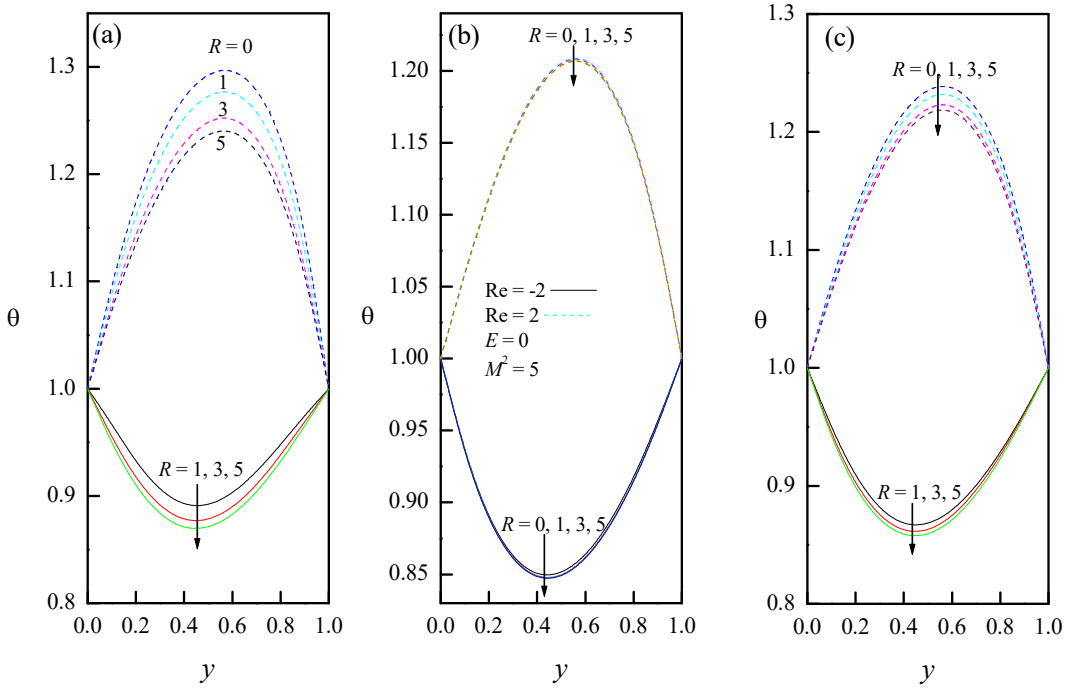

Fig. 7. Temperature for different values of micropolar parameter, electric load parameter, and Reynolds number with $M^2=5$, $A=1$, $B=0.001$, $q=1$, $\mathrm{Pr}=0.733$, $\varepsilon=1$, $\gamma=1$.

The effect of micropolar parameter and the electric load parameter on the microrotation velocity is shown in Fig. 6. As the micropolar parameter increases, the microrotation velocity decreases in the left half of the region and increases in the right half of the region for $E=-1$ and 0 m, whereas the microrotation velocity increases in the left half of the region and increases in the right half of the region. The microrotation velocity is higher in the left half of the region and lower in the right half of the region for suction as compared to injection for both open and short circuits.

The effect of micropolar parameter and electric load parameter on the temperature is shown in Fig. 7. As the micropolar parameter increases, the temperature decreases for both injection and suction. Moreover, in this case, the temperature is higher

for suction as compared to injection. It is observed in Fig. 6 that the temperature is invariant for the short circuit as compared to the open circuit. Since the temperature distribution depends upon ε, therefore, for $\mathrm{Re} < 0$, it increases and attains a maximum and then decreases.

The skin friction and couple stresses have been given for $\mathrm{Re} = -2$ and 2 in Figs. 8a and 8b, respectively, which show their variation with respect to the Hartmann number M^2 for a fixed value of the micropolar parameter. From the Fig. 8, it is noticed that the skin friction and couple stresses decrease with the increase in Hartmann number at both walls for both injection and suction. Moreover, it is observed that at the left wall, the skin friction is predominating for suction whereas at the right wall, the injection is predominating. The effect of micropolar parameter on the skin friction and couple stresses is shown in Fig. 9 for fixed Hartmann number $M^2 = 5$. As the micropolar parameter increases, the skin friction at the right wall decreases whereas the skin friction at the left wall increases as can be seen in Fig. 9a. It is observed that the skin friction is more effective for suction as compared to injection. The micropolar parameter decreases the couple stresses at both walls for injection and suction as can be seen in Fig. 9b.

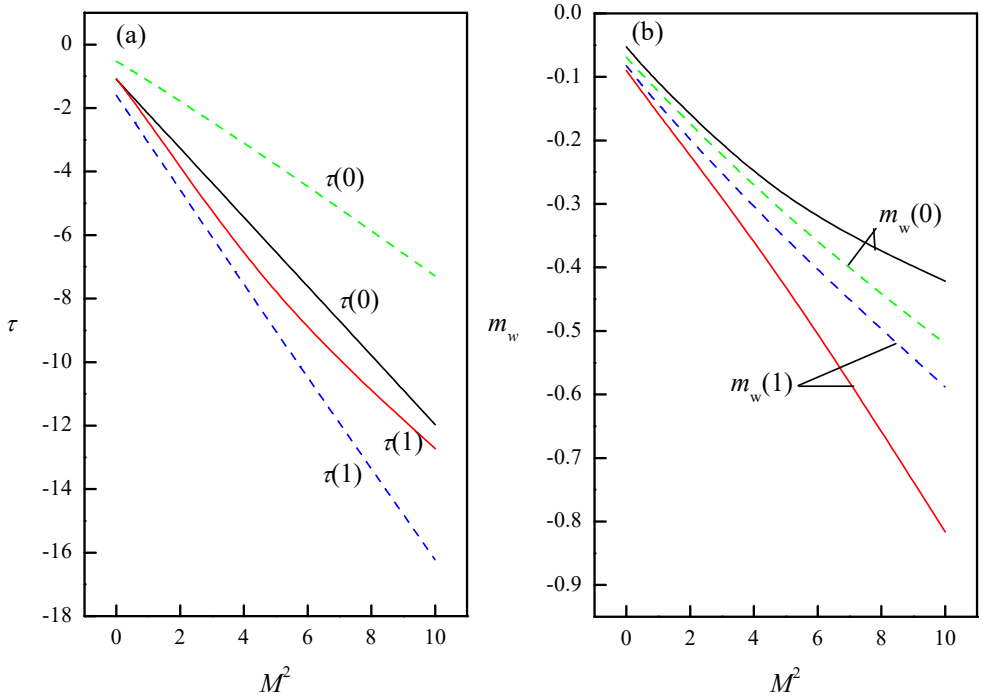

Fig. 8. Skin friction and couple stresses for different values of Hartmann number and Reynolds number with $M^2 = 5$, $E = -1$, $A = 1$, $B = 0.001$, $q = 1$, $\mathrm{Pr} = 0.733$, $\varepsilon = 1$, $\gamma = 1$.

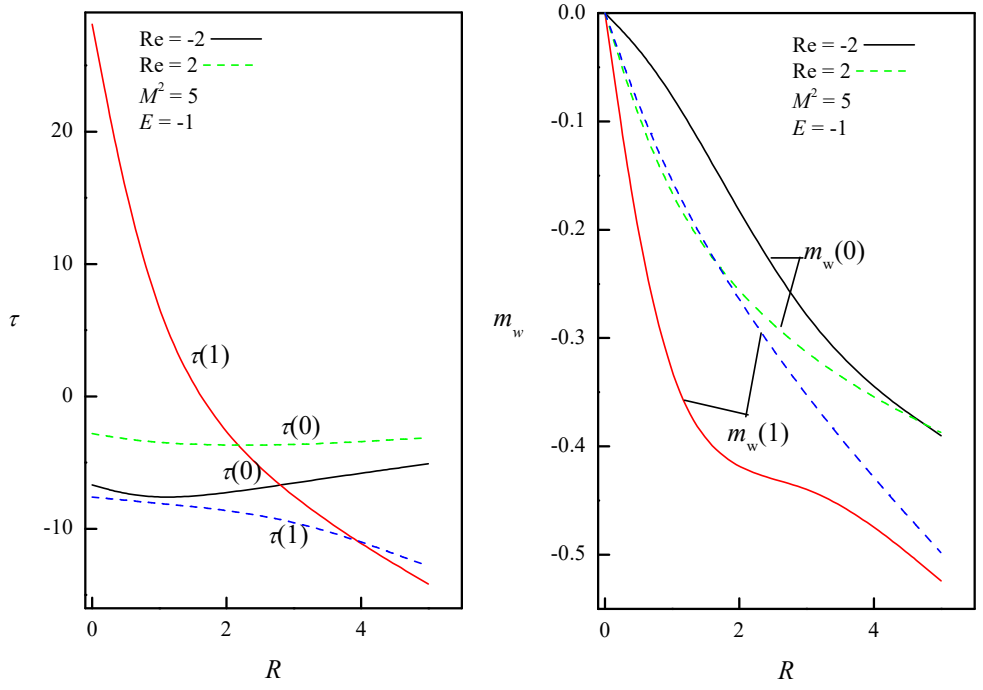

Fig. 9. Skin friction and couple stresses for different values of micropolar parameter and Reynolds number with $M^2 = 5$, $E = -1$, $A = 1$, $B = 0.001$, $q = 1$, $\mathrm{Pr} = 0.733$, $\varepsilon = 1$, $\gamma = 1$.

Figures 10a and 10b show the effect of Hartmann number M^2 and micropolar parameter R on Nusset number on both walls. It is observed that as the Hartmann number increases, the Nusselt number $Nu(0)$ at the left wall decreases whereas Nusselt number $Nu(1)$ at the right wall increases for both injection and suction as can be seen in Fig. 10a. It is also seen in Fig. 10a that the Nusselt number is more effective for injection as compared to suction. As the micropolar parameter R increases, the Nusselt number $Nu(0)$ at the left wall increases whereas the Nusselt number $Nu(1)$ at the right wall decreases and become constant at $R > 4$ for injection as can be seen in Fig. 10b. Moreover, in this case, the Nusselt number is more effective for injection when compared to suction.

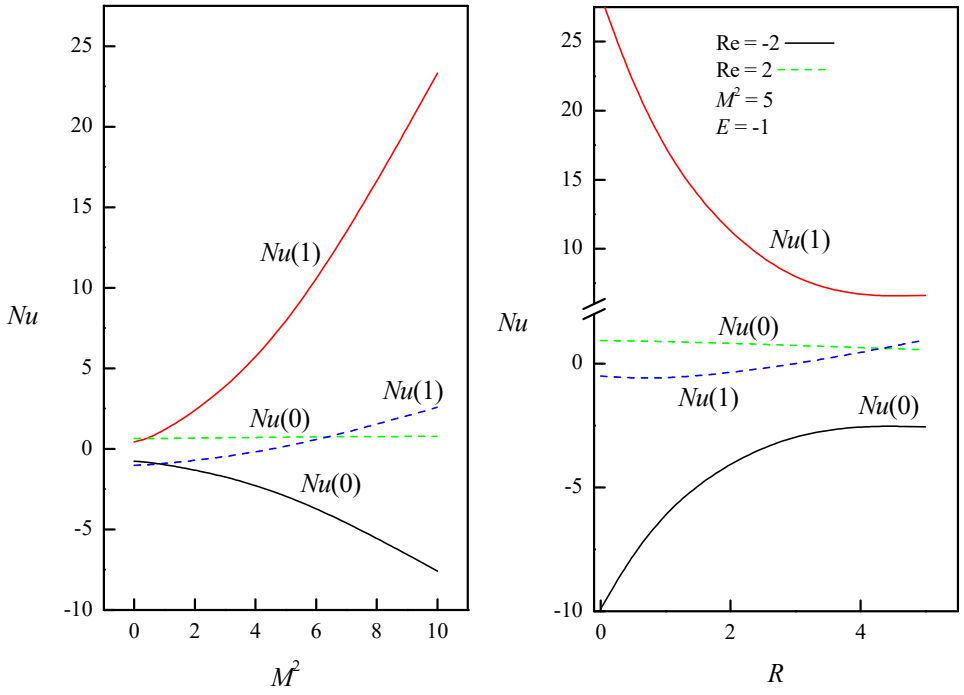

Fig. 10. Nusselt number for different values of (a) Hartmann number (b) micropolar parameter and Reynolds number with $M^2 = 5$, $E = -1$, $A = 1$, $B = 0.001$, $q = 1$, $\Pr = 0.733$, $\varepsilon = 1$, $\gamma = 1$.

5. Conclusion

In this study, the effect of temperature-dependent heat sources on the fully developed free convection electrically conducting micropolar fluid between two parallel porous vertical plates in a strong cross magnetic field was investigated. The solutions were obtained from DTM, and indicated what these solutions mean in terms of the relative importance of the various micropolar parameters on this kind of flow prediction. Complementary numerical solutions were obtained via Runge – Kutta shooting method and a very excellent agreement between the solutions obtained from DTM and the computations was observed for suction. Moreover, the results of velocity and temperature gradient were compared with Bhargava et al. [16] and a good agreement between the results was observed for both suction and injection in the absence of applied electric field. After ensuring the validity, results were given for the velocity, microrotation, and temperature for various values of governing parameters. It was found that the increase in the Hartmann number had different effects on velocity, microrotation, and temperature. The micropolar parameter reduced the velocity and the temperature whereas enhanced the microrotation in the half of the region. The Hartmann number and the micropolar parameter decreases the skin friction and couple stresses. The Nusselt number increased with the Hartmann number on the right wall and decreased on the left wall whereas the micropolar parameter decreased the Nusselt number on the right wall and increases on the left wall. The results were in good agreement with Bhargava et al. [16] and the existing numerical results and therefore elucidated the reliability and efficiency of DTM. The comparisons made suggested that the DTM could be a useful and effective tool in solving systems of nonlinear differential equations of the micropolar flow through the porous channel walls with applied electric and magnetic fields.

References

[1] A.C. Eringen, Theory of micropolar fluids, *Journal of Mathematics and Mechanics*, 16, 1966, 1–18.
[2] A.C. Eringen, Theory of thermomicrofluids, *Journal of Mathematical Analysis and Applications*, 38, 1972, 480–496.
[3] G. Lukaszewicz, *Micropolar fluids: theory and applications*, Birkhauser, Basel, 1999.
[4] A.C. Eringen, *Microcontinuum field theories, II. Fluent media*, Springer, New York, 2001.
[5] T. Ariman, M.A. Turk, N.D. Sylvester, Micro continuum fluid mechanics – A review, *International Journal of Engineering Science*, 11, 1973, 905–930.

[6] R.S. Agarwal, C. Dhanapal, Numerical solution of free convection micropolar fluid flow between two parallel porous vertical plates, *International Journal of Engineering Science*, 26, 1988, 1247–1255.
[7] D. Srinivasacharya, J.V. Ramana Murthy, D. Venugopalam, Unsteady stokes flow of micropolar fluid between two parallel porous plates, *International Journal of Engineering Science*, 39, 2001, 1557–1563.
[8] M.F. El-Amin, Magnetohydrodynamic free convection and mass transfer flow in micropolar fluid with constant suction, *Journal of Magnetism and Magnetic Materials*, 234, 2001, 567–574.
[9] M.F. El-Amin, Combined effect of internal heat generation and magnetic field on free convection and mass transfer flow in a micropolar fluid with constant suction, *Journal of Magnetism and Magnetic Materials*, 270, 2004, 130–135.
[10] M. Emad, A.F. Abo-Eldahab, Ghonaim, Convective heat transfer in an electrically conducting micropolar fluid at a stretching surface with uniform free stream, *Applied Mathematics and Computation*, 137, 2003, 323–336.
[11] A.A. Joneidi, D.D. Ganji, M. Babaelahi, Micropolar flow in a porous channel with high mass transfer, *International Communications in Heat and Mass Transfer*, 36, 2009, 1082-1088.
[12] J. Prathap Kumar, J.C. Umavathi, Ali J. Chamkha, Ioan Pop, Fully-developed free-convective flow of micropolar and viscous fluids in a vertical channel, *Applied Mathematical Modelling*, 34, 2010, 1175–1186.
[13] R. Mahmood, M. Sajid, Flow of a micropolar fluid through two parallel porous boundaries, *Numerical Methods for Partial Differential Equations*, 27, 2011, 637–643.
[14] M.A. El-Haikem, A.A. Mohammadein, S.M.M. El-Kabeir, Joule heating effects on magnetohydrodynamic free convection flow of a micropolar fluid, *International Communications in Heat and Mass Transfer*, 2, 1999, 219.
[15] M.F. El-Amin, Magnetohydrodynamic free convection and mass transfer flow in micropolar fluid with constant suction, *Journal of Magnetism and Magnetic Materials*, 234, 2001, 567.
[16] R. Bhargava, L. Kumar, H.S. Takhar, Numerical solution of free convection MHD micropolar fluid flow between two parallel porous vertical plates, *International Journal of Engineering Science*, 41, 2003, 123–136.
[17] J. Zueco, P. Eguía, L.M. López-Ochoa, J. Collazo, D. Patiño, Unsteady MHD free convection of a micropolar fluid between two parallel porous vertical walls with convection from the ambient, *International Communications in Heat and Mass Transfer*, 36, 2009, 203–209
[18] J.C. Umavathi, I.C. Liu, J. Prathap Kumar, Magnetohydrodynamic Poseuille-Coutte flow and heat transfer in an inclined channel, *Journal of Mechanics*, 26, 2010, 525-532.
[19] A.T. Akinshilo, J.O. Olofinkua, O. Olaye, Flow and heat transfer analysis of the Sodium Alginate conveying Copper Nanoparticles between two parallel plates, *Journal of Applied and Computational Mechanics*, 3, 2017, 258-266.
[20] A.T. Akinshilo, G.M. Sobamowo, Perturbation solutions for the study of MHD blood as a third grade nanofluid transporting gold nanoparticles through a porous channel, *Journal of Applied and Computational Mechanics*, 3, 2017, 103-113.
[21] E. Ghahremani, R. Ghaffari, H. Ghadjari, J. Mokhtari, Effect of variable thermal expansion coefficient and nanofluid properties on steady natural convection in an enclosure, *Journal of Applied and Computational Mechanics*, 3, 2017, 240-250
[22] A. Noghrehabadi, R. Pourrajab, M. Ghalambaz, Effect of partial slip boundary condition on the flow and heat transfer of nanofluids past stretching sheet prescribed constant wall temperature, *International Journal of Thermal Sciences*, 54, 2012, 253-261.
[23] A. Noghrehabadi, M.R. Saffarian, R. Pourrajab, M. Ghalambaz, Entropy analysis for nanofluid flow over a stretching sheet in the presence of heat generation/absorption and partial slip, *Journal of Mechanical Science and Technology*, 27, 2013, 927-937.
[24] H. Zargartalebi, A. Noghrehabadi, M. Ghalambaz, I. Pop, Natural convection boundary layer flow over a horizontal plate embedded in a porous medium saturated with a nanofluid: case of variable thermophysical properties, *Transport in Porous Media*, 107, 2015, 153-170.
[25] A. Noghrehabadi, M. Ghalambaz, A. Ghanbarzadeh, A new approach to the electrostatic pull-in instability of nanocantilever actuators using the ADM- Padé technique, *Computers and Mathematics with Applications*, 64, 2012, 2806-2815.
[26] J.K. Zhou, *Differential transformation and its applications for electrical circuits*, Huazhong University Press, 1986.
[27] C.K. Chen, S.H. Ho, Solving partial differential equations by two dimensional differential transform method, *Applied Mathematics and Computation*, 106, 1999, 171–179.
[28] F. Ayaz, Solutions of the systems of differential equations by differential transform method, *Applied Mathematics and Computation*, 147, 2004, 547–567.
[29] A.S.V. Ravi Kanth, K. Aruna, Solution of singular two-point boundary value problems using differential transformation method, *Physics Letters A*, 372, 2008, 4671–4673.
[30] I.H. Abdel-Halim Hassan, Comparison differential transformation technique with Adomian decomposition method for linear and nonlinear initial value problems, *Chaos, Solitons and Fractals*, 36, 2008, 53–65.
[31] M.J. Jang, C.L. Chen, Y.C. Liu, Two-dimensional differential transform for partial differential equations, *Applied Mathematics and Computation*, 121, 2001, 261–270.
[32] D.D. Ganji, H. Bararnia, S. Soleimani, E. Ghasemi, Analytical solution of the magneto-hydrodynamic flow over a nonlinear stretching sheet, *Modern Physics Letters* B, 23, 2009, 2541–2556.
[33] A. Kurnaz, G. Oturnaz, M.E. Kiris, n-Dimensional differential transformation method for solving linear and nonlinear PDE's, *International Journal of Computer Mathematics*, 82, 2005, 369–380.
[34] M.M. Rashidi, E. Erfani, New analytical method for solving Burgers' and nonlinear heat transfer equations and comparison with HAM, *Computer Physics Communications*, 180, 2009, 1539–1544.
[35] J.C. Umavathi, A.S.V. Ravi Kanth, and M. Shekar, Comparison study of differential transform method with finite difference method for magneto convection in a vertical channel, *Heat Transfer-Asian Research*, 42(3), 2013, 243–258.